JOURNAL OF Materials CHEMISTRY

Layered $Li_xMn_{1-y}Ni_yO_2$ intercalation electrodes

Tracey E. Quine, Morven J. Duncan, A. Robert Armstrong, Alastair D. Robertson and Peter G. Bruce*

School of Chemistry, University of St. Andrews, St. Andrews, Fife, UK KY16 9ST. E-mail: pgb1@st-and.ac.uk

Received 19th July 2000, Accepted 22nd September 2000
First published as an Advance Article on the web 7th November 2000

Synthesis of the layered lithium intercalation compound $Li_xMn_{1-y}Ni_yO_2$, with the O3 (α-$NaFeO_2$) structure is reported and it is shown to exhibit amongst the highest capacity to cycle lithium (charge) on intercalation/deintercalation (220 mA h g^{-1} between potential limits of 2.4 to 4.8 V) of any such material and at a relatively high charge/discharge rate; the ion exchange conditions used in the synthesis have an important influence on the defect chemistry of the host structure and this in turn influences the performance of the compound as an electrode in rechargeable lithium batteries.

Introduction

The investigation of materials for rechargeable lithium batteries has now become a major topic of materials research world-wide, driven in part by the recent growth of lithium battery technology. One of the key and urgent challenges facing the advancement of rechargeable lithium batteries is the need to replace $LiCoO_2$ based positive electrodes with lithium intercalation compounds that are cheaper, less toxic, safer and can store more charge (lithium) on charge/discharge cycling. Lithium manganese oxide based compounds are particularly attractive in this regard. The non-stoichiometric spinel $Li_{1+x}Mn_{2-x}O_4$ has already been studied extensively and possesses a discharge capacity of 120 mA h g^{-1}, somewhat less than $LiCoO_2$ (130 mA h g^{-1}).[1–6] Recently, layered $LiMnO_2$ with the O3 (α-$NaFeO_2$) structure has been successfully synthesised by an ion exchange route and can act as an intercalation host for lithium.[7,8] The stoichiometric compound converts to spinel on cycling and can sustain only a modest capacity to store charge corresponding to $\sim$130 mA h g^{-1}.[9,10] Doping with for example Co or Al slows but does not stop conversion to spinel; however, it does lead to improved capacity retention on cycling.[11–15]

In this paper we investigate layered $LiMnO_2$ doped with Ni, restricting our attention to materials with up to 20% substitution of Mn by Ni. Such materials could prove interesting and potentially attractive cathode materials because both Mn and Ni are cheaper than Co. By investigating Mn rich compositions the problems of capacity fade and safety, anticipated for Ni rich materials based on the known behaviour of $LiNiO_2$,[16–20] will be avoided. Lithium manganese nickel oxides with other layered structures, in particular O2, have recently been described.[21]

Experimental

Preparation

Layered $Na_xMn_{1-y}Ni_yO_2$ was prepared by adding a solution of Na_2CO_3 (Aldrich, 99.5%) in distilled water to an aqueous solution of $Mn(CH_3CO_2)_2{\cdot}4H_2O$ (Aldrich, 99%+) and $Ni(CH_3CO_2)_2{\cdot}4H_2O$ (Aldrich, 98%).[22] Stoichiometric quantities of the reagents were used (including 1 Na per formula unit, *i.e.* $x=1$) and the acetates were completely dissolved by heating their solutions to 80 °C. Following mixing and rotary evaporation at 80 °C the powders were heated in air, first at 200 °C for 12 h followed by 600 °C for 1 h then quenched to room temperature. The resulting sodium phases were ion exchanged using an excess of LiBr under three different conditions, refluxing at 160 °C for 6–8 h in hexanol, refluxing at 80 °C for 6–8 h in ethanol or exchange at 25 °C for 1 week in ethanol. Following these procedures the solids were filtered and washed with ethanol and water before drying.

Characterisation

Structural characterisation was carried out using powder X-ray diffraction on a Stoe STADI/P diffractometer operating in transmission mode and with a Fe source ($\lambda=1.93604$ Å) to avoid fluorescence. Neutron diffraction data were collected on the GEM diffractometer at the Rutherford Appleton Laboratory. The structures were refined by the Rietveld method using the program TF12LS based on the Cambridge Crystallographic Subroutine Library (CCSL).[23,24] Neutron scattering lengths of -0.19, -0.373, 1.03 and 0.5803 (all $\times 10^{-12}$ cm) were assigned to Li, Mn, Ni and O respectively.[25] Chemical analysis was carried out by flame emission and atomic absorption spectroscopy on a PU 9400 instrument, the former technique was used for the alkali metals and the latter for the transition metals. The Na content of the Na phase was determined by subtraction of the Na_2CO_3 content, the latter being measured by carbon microanalysis. Oxidation states were determined using a Mettler DL 40 RC auto titrator, the sample was digested in an excess of ferrous ammonium sulfate solution and then titrated with standardised $KMnO_4$.[26] Further investigation of the nickel oxidation states was carried out using XPS on a VG ESCALAB 3 instrument. Non-stoichiometric nickel oxide ($Ni_{1-x}O$) was used as a standard for both Ni^{2+} and Ni^{3+}. Surface areas were determined to be $\sim$10 m^2 g^{-1} by BET measurements using a Micromeritics Gemini 23670 instrument. Electrodes were fabricated using the Doctor Blade technique. This involved mixing active material, super S carbon and Kynar Flex 2801 in the weight ratios 85 : 10 : 5 in a solution of THF. This mixture was spread on to aluminium foil which was then dried under vacuum overnight at 70 °C before incorporation into an electrochemical cell in which the second electrode was lithium metal and the electrolyte was a 1 molal solution of $LiPF_6$ in PC. Electrochemical measurements were carried out using a BioLogic MacPile multichannel cycler.

 DOI: 10.1039/b007429m

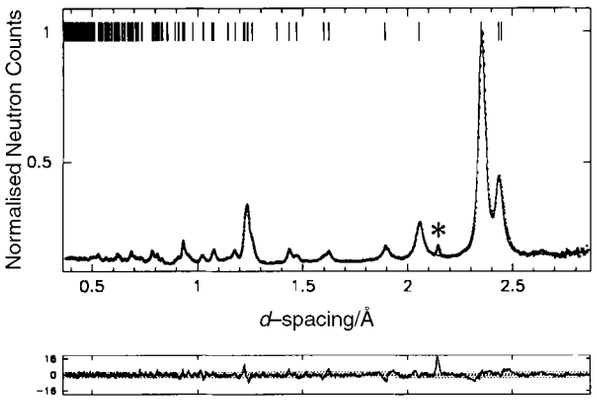

Fig. 1 Powder neutron diffraction pattern for 5% Ni doped layered lithium manganese oxide ion exchanged in ethanol at 80 °C. Dots: experimental points, solid line: best fit, lower curve: difference plot. Peak marked by * corresponds to the vanadium container.

Table 1 Lattice parameters for layered lithium manganese oxide materials doped with 2.5%, 5%, 7.5%, 10% and 20% Ni under three different ion exchange conditions

Ni Content	Ion exchange	*a*/Å	*c*/Å	*c*/*a*
0.025	Ethanol, 25 °C	2.8658(8)	14.6913(26)	5.13
	Ethanol, 80 °C	2.8712(9)	14.6145(21)	5.09
	Hexanol, 160 °C	2.8895(7)	14.4802(13)	5.01
0.05	Ethanol, 25 °C	2.8656(4)	14.6954(24)	5.13
	Ethanol, 80 °C	2.8663(2)	14.5904(14)	5.09
	Hexanol, 160 °C	2.8873(5)	14.3989(24)	4.99
0.075	Ethanol, 25 °C	2.8626(4)	14.6515(23)	5.12
	Ethanol, 80 °C	2.8659(0)	14.6084(16)	5.10
	Hexanol, 160 °C	2.8840(9)	14.4152(21)	5.00
0.1	Ethanol, 25 °C	2.8633(4)	14.6358(31)	5.11
	Ethanol, 80 °C	2.8683(3)	14.6283(16)	5.10
	Hexanol, 160 °C	2.8761(3)	14.4176(16)	5.01
0.2	Ethanol, 25 °C	2.8697(8)	14.6465(17)	5.10
	Ethanol, 80 °C	2.8714(3)	14.6001(19)	5.09
	Hexanol, 160 °C	2.8864(4)	14.4746(37)	5.01

Results and discussion

Structure and composition

Considering first the sodium phases with nickel substitution, powder X-ray diffraction patterns revealed that, under the synthesis conditions used here, the layered phase is always accompanied by some unreacted Na_2CO_3, implying that the main phase must contain less than 1 sodium per formula unit. Following ion exchange and washing, powder X-ray and neutron diffraction patterns indicate that the Na_2CO_3 had been successfully removed and only a single lithium phase remained. A powder neutron diffraction pattern for the lithium phase with 5% Ni and ion exchanged in ethanol at 80 °C, is shown in Fig. 1. Regardless of ion exchange conditions the diffraction patterns may be indexed based on the layered rhombohedral (O3) structure of $LiCoO_2$ (α-$NaFeO_2$ structure type) in space group $R\bar{3}m$.

The layered phases are not identical, as is evident from Table 1 which reports the lattice parameters for different ion exchange conditions and Ni contents. XPS results indicate that Ni is in the divalent state implying that the solid solution mechanism requires replacement of $2Mn^{3+}$ by a Mn^{4+} and Ni^{2+} ion. This involves a change in the average ionic radius from 0.645 Å, for high spin Mn^{3+}, to 0.610 Å, for Mn^{4+}/Ni^{2+}. Since the change in the average ionic radius is relatively small there will only be a small shift in the transition metal to oxygen bond length for substitution levels up to 20% and this is consistent with the relative invariance of *a* with Ni content (the *a* parameter lies in the basal plane).

More interesting is the variation in lattice parameters with ion exchange conditions. It is clear that both the *a* and *c* lattice parameters vary with ion exchange temperature such that *a* decreases and *c* increases as the ion exchange temperature is reduced. An indication of the origins of these variations may be obtained by examining the chemical analysis presented in Table 2. Since the differences in the lattice parameters are mainly between the materials prepared by refluxing in ethanol and hexanol we focus attention on the compositions of materials prepared under these two conditions and for three nickel doping levels to illustrate the trends. All the materials are alkali metal deficient, originating from the Na deficiency of the phases prior to exchange. In the hexanol samples essentially all the Na has been exchanged with Li whereas some Na remains after refluxing in ethanol. Of particular note is the presence of vacancies on the transition metal sites, such vacancies are always greater for the lower temperature reflux and in most of the cases studied there are essentially no transition metal vacancies after refluxing in hexanol at 160 °C. The greater level of transition metal vacancies coupled with the lower overall alkali metal content in the case of the samples prepared in ethanol conspires to produce a higher average Mn oxidation state for the ethanol samples. As a result a shorter average TM–O bond length is expected with an associated reduction in the *a* lattice parameter as observed. The trends in composition, particularly the lower alkali metal content for ethanol samples, are consistent with the longer *c* axis (lower alkali metal content frequently give rise to longer *c* axes in layered oxides due to the weak van der Waal's bonding). The somewhat greater Na^+ ion content in the ethanol samples may also contribute to the larger *c* axis since Na^+ has a larger ionic radius than Li^+ (1.02 Å *vs.* 0.76 Å, respectively).

Analysis of the sodium phases prior to exchange reveals that they too possess vacancies on the transition metal sites. Such cation vacancies inevitably carry, in the language of defect chemistry introduced by Kröger-Vink,[27] a negative effective charge which will trap a proportion of the Na^+ ions rendering them relatively immobile and difficult to exchange. It is therefore not a coincidence that the persistence of transition metal vacancies in the materials exchanged in ethanol is accompanied by incomplete exchange of Na^+ by Li^+. Refluxing in hexanol at 160 °C however, is sufficiently reducing to promote elimination of transition metal vacancies and as a result the Na^+ ions are not trapped leading to complete exchange of Na by Li. Clearly the ion exchange process can alter the structure, defect structure and composition of these layered materials. It may also be noted that the conditions are

Table 2 Chemical analysis for layered manganese oxide materials doped with 5%, 7.5% and 10% Ni

Ni Content	Ion exchange	Stoichiometry	TM vacancies	Average Mn oxidation state
0.05	Ethanol, 80 °C	$Na_{0.029}Li_{0.68}Mn_{0.88}Ni_{0.045}O_2$	7%	3.63
	Hexanol, 160 °C	$Na_{0.011}Li_{0.75}Mn_{0.93}Ni_{0.048}O_2$	2%	3.38
	Na phase	$Na_{0.42}Mn_{0.88}Ni_{0.077}O_2$	4%	3.89
0.075	Ethanol, 80 °C	$Na_{0.021}Li_{0.60}Mn_{0.87}Ni_{0.070}O_2$	6%	3.72
	Hexanol, 160 °C	$Na_{0.010}Li_{0.65}Mn_{0.92}Ni_{0.073}O_2$	0%	3.47
0.1	Ethanol, 80 °C	$Na_{0.030}Li_{0.55}Mn_{0.87}Ni_{0.089}O_2$	4%	3.73
	Hexanol, 160 °C	$Na_{0.010}Li_{0.68}Mn_{0.92}Ni_{0.096}O_2$	0%	3.39

Table 3 Crystallographic data for $Li_xMn_{0.95}Ni_{0.05}O_2$ refluxed in ethanol at 80 °C[a]

Atom	Wyckoff symbol	*x*/*a*	*y*/*a*	*z*/*c*	B_{iso}	Occupancy
Li/Na	3b	0.0	0.0	0.5	0.75 (14)	0.672(14)/0.029
Mn/Ni[b]	3a	0.0	0.0	0.0	—	0.871(9)/0.045
O1[c]	6c	0.0	0.0	0.26211(6)	—	1

[a]Space group $R\bar{3}m$, $a=2.8663(2)$ Å, $c=14.5904(6)$ Å, $R_{exp}=1.1\%$, $R_{wP}=2.0\%$, $R_P=1.8\%$. $R_I=2.3\%$. [b]Mn/Ni: $B_{11}=B_{22}=1.2(1)$, $B_{33}=1.9(2)$, $B_{12}=0.60(5)$. [c]O1: $B_{11}=B_{22}=0.71(1)$, $B_{33}=0.98(3)$, $B_{12}=0.36(1)$.

sufficiently reducing in both ethanol and hexanol to promote some Li intercalation along with exchange, as is evident by comparison of the alkali metal content before and after exchange.

The structure of the layered materials was probed further by Rietveld refinement based on the neutron diffraction data. Of particular interest are the defect layered compounds with vacancies on the transition metal sites. If we consider the data in Fig. 1 for the 5% nickel doped material refluxed in ethanol at 80 °C, an excellent fit to the data may be obtained based on the layered O3 structure, $R\bar{3}m$. In this structural model the oxide ions adopt a cubic close packed arrangement with Mn and Ni together partially occupying alternate sheets of octahedral (3a) sites. The alkali metal ions partially occupy the remaining sheets of octahedral sites (3b). The Rietveld refinement was carried out with the Na and Ni contents fixed at the values obtained from the chemical analysis, and the Li and Mn occupancies were allowed to vary freely. Crystallographic data and *R* factors are given in Table 3. It is evident that the refined Li and transition metal vacancy contents are in good agreement with the chemical analysis.

Electrochemistry

Turning to the electrochemical performance, the influence of the ion exchange conditions on the variation of discharge capacity with cycle number is shown in Fig. 2. In general, the materials prepared in hexanol lose capacity more rapidly than those synthesised in ethanol. Ion exchange at 80 °C gives rise to materials with a somewhat higher capacity than those prepared at room temperature.

For materials prepared at 80 °C in ethanol, a comparison of discharge capacities for different Ni doping levels is shown in Fig. 3. The initial discharge capacities are quite similar, however, some variation is evident after a number of cycles. For example, comparing different materials after ten cycles, the capacity increases with nickel doping up to 5% then decreases thereafter. Considering all the compositions and ion exchange conditions studied, the best combination of high capacity and good capacity retention (99.8% per cycle) is obtained for the 5% nickel doped material prepared at 80 °C in ethanol.

A complete understanding of the trends in capacity retention as a function of Ni content on reflux conditions is not yet available. We and others have however discussed the significance of forming a nanostructured material on cycling such layered compounds and the role this can play in facilitating Li cycling.[9,28] It may be that the nanostructures derived from materials refluxed under different conditions or with different Ni contents possess variations that have a significant influence on cycling.

Voltage profiles for the material which exhibits the best performance are shown in Fig. 4. A capacity of around 220 mA h g^{-1} is delivered above 2.5 V by $Li_xMn_{0.95}Ni_{0.05}O_2$ prepared at 80 °C in ethanol. The rate capability of the material is also demonstrated in Fig. 4 where the discharge profile at 50 mA g^{-1} (approximately *C*/4) is shown. Doubling the rate leads to only a modest reduction in the discharge capacity with the material still delivering 200 mA h g^{-1} in the voltage range 2.4–4.8 V. In the future, rechargeable lithium ion batteries will find a major market in electronic devices operating at below 2 V for which batteries operating at or above this voltage will be required. The 5% Ni doped material reported here delivering 220 mA h g^{-1} at *C*/8 and 200 mA h g^{-1} at a rate of *C*/4 (2.4 to 4.8 V) represents an interesting development in the context of new positive electrodes for rechargeable lithium batteries.

It is well known that layered $LiMnO_2$ and materials lightly doped with Co or Al transform to spinel-like phases on cycling[11–14] and the Ni doped materials reported here are no exception. Powder X-ray diffraction data collected after 10 and 24 cycles on a 5% Ni doped material prepared in hexanol at

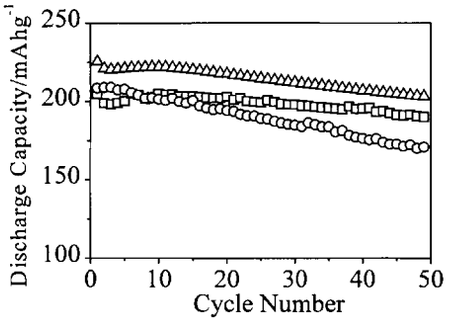

Fig. 2 Discharge capacities as a function of cycle number for 5% Ni doped material exchanged under the three different conditions: ethanol 25 °C (□), ethanol 80 °C (△), hexanol 160 °C (○). Rate = 25 mA g^{-1} (*C*/8). Potential range 2.4–4.8 V, 30 °C.

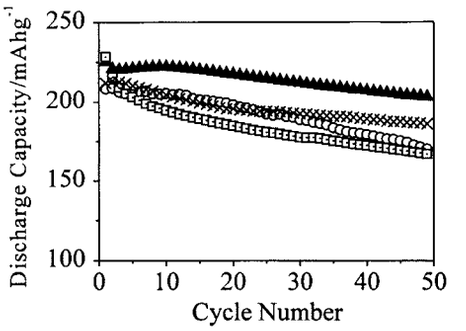

Fig. 3 Comparison of discharge capacities for $Li_xMn_{1-y}Ni_yO_2$ materials prepared in ethanol at 80 °C, $y=0.025$ (X), $y=0.05$ (▲), $y=0.075$ (○), $y=0.2$ (□). Rate = 25 mA g^{-1} (*C*/8). Potential range 2.4–4.8 V, 30 °C.

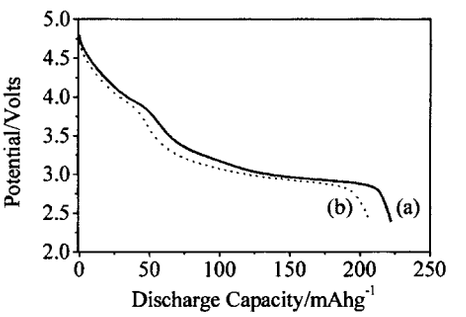

Fig. 4 Discharge voltage *vs.* state of charge at two different current densities for 5% Ni doped material refluxed in ethanol at 80 °C after 10 cycles, 30 °C: (a) 25 mA g^{-1} (*C*/8) —, (b) 50 mA g^{-1} (*C*/4) ------.

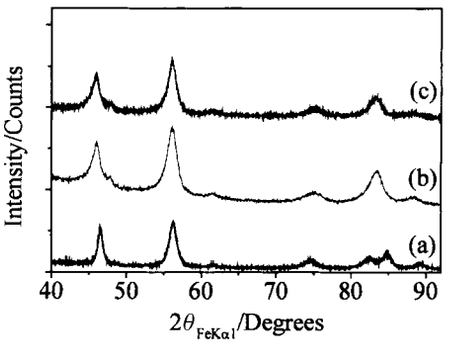

Fig. 5 Powder X-ray diffraction patterns for 5% Ni doped material exchanged in ethanol at 80 °C: (a) as-prepared, (b) after 24 cycles and (c) after 10 cycles but exchanged in hexanol at 160 °C.

160 °C and ethanol at 80 °C, respectively are shown in Fig. 5. In both cases, the data are consistent with a spinel-like structure. In the former case, transformation to spinel is essentially complete within 10 cycles, whereas in the latter this occurs after more than 20 cycles. In general, the lower temperature reflux conditions slow the conversion to spinel.

In summary, it is evident that varying the ion exchange conditions has a key influence on the structure and composition of the layered lithium manganese oxides doped with nickel. These differences in composition and particularly in defect structure lead to important differences in the electrochemical performance of the materials. The materials can exhibit high capacities and good retention of these capacities on cycling.

Acknowledgements

P.G.B. is indebted to the EPSRC for financial support and to SF/NVR for the XPS measurements. T.E.Q. is grateful for the support of an EPSRC studentship.

References

1 M. M. Thackeray, *J. Electrochem. Soc.*, 1995, **142**, 2558and references therein.
2 J. M. Tarascon, W. R. McKinnon, F. Coowar, T. N. Bowmer, G. Amatucci and D. Guyomard, *J. Electrochem. Soc.*, 1994, **141**, 1421.
3 Y. Gao and J. R. Dahn, *J. Electrochem. Soc.*, 1996, **143**, 100.
4 J. M. Tarascon, E. Wang, F. K. Shokoohi, W. R. McKinnon and S. Colson, *J. Electrochem. Soc.*, 1991, **138**, 2859.
5 G. Pistoia, A. Antonini, R. Rosati, C. Bellitto and G. M. Ingo, *Chem. Mater.*, 1997, **9**, 1443.
6 A. D. Robertson, S. H. Lu, W. F. Averill and W. F. Howard Jr, *J. Electrochem. Soc.*, 1997, **144**, 3500; A. D. Robertson, S. H. Lu, W. F. Averill and W. F. Howard Jr., *J. Electrochem. Soc.*, 1997, **144**, 3505.
7 A. R. Armstrong and P. G. Bruce, *Nature*, 1996, **381**, 499.
8 F. Capitaine, P. Gravereau and C. Delmas, *Solid State Ionics*, 1996, **89**, 197.
9 P. G. Bruce, A. R. Armstrong and R. L. Gitzendanner, *J. Mater. Chem.*, 1999, **9**, 193.
10 G. Vitins and K. West, *J. Electrochem. Soc.*, 1997, **144**, 2587.
11 A. R. Armstrong, R. L. Gitzendanner, A. D. Robertson and P. G. Bruce, *Chem. Commun.*, 1998, 1833.
12 A. R. Armstrong, A. D. Robertson, R. L. Gitzendanner and P. G. Bruce, *J. Solid State Chem.*, 1999, **145**, 549.
13 A. R. Armstrong, A. D. Robertson and P. G. Bruce, *Electrochim. Acta*, 1999, **45**, 285.
14 Y.-I. Jang, B. Huang, H. Wang, Y.-M. Chiang and D. R. Sadoway, *Electrochem. Solid State Lett.*, 1998, **1**, 13.
15 G. Ceder, Y.-M. Chiang, D. R. Sadoway, M. K. Aydinol, Y.-I. Jang and B. Huang, *Nature*, 1998, **392**, 694.
16 J. R. Dahn, U. von Sacken, M. W. Juzkow and H. Al-Janaby, *J. Electrochem. Soc.*, 1991, **138**, 2207.
17 T. Ohzuku, A. Ueda and M. Nagayama, *J. Electrochem. Soc.*, 1993, **140**, 1862.
18 M. Broussely, F. Perton, P. Beinsan, J. M. Bodet, J. Labat, A. Lecerf, C. Delmas, A. Rougier and J. P. Pérès, *J. Power Sources*, 1995, **54**, 109.
19 A. Rougier, P. Gravereau and C. Delmas, *J. Electrochem. Soc.*, 1996, **143**, 1168.
20 J. R. Dahn, E. W. Kuller, M. Obrovac and U. Vonsacken, *Solid State Ionics*, 1994, **69**, 265.
21 J. M. Paulsen, C. L. Thomas and J. R. Dahn, *J. Electrochem. Soc.*, 2000, **147**, 861.
22 For preparation of 5% Ni doped Na-phase: 3.18 g of Na_2CO_3 dissolved in 100 ml of distilled water was added to a 200 ml solution containing 13.97 g of $Mn(CH_3CO_2)_2{\cdot}4H_2O$ and 0.74 g of $Ni(CH_3CO_2)_2{\cdot}4H_2O$.
23 J. C. Matthewman, P. Thompson and P. J. Brown, *J. Appl. Crystallogr.*, 1982, **15**, 167.
24 P. J. Brown and J. C. Matthewman, Rutherford Appleton Laboratory Report, RAL-87-010, 1987.
25 V. F. Sears, *Neutron News*, 1992, **3**, 26.
26 M. J. Katz, R. C. Clarke and W. F. Nye, *Anal. Chem.*, 1956, **28**, 507.
27 R. J. D. Tilley, *Defect Crystal Chemistry and its Applications*, Blackie Academic Publishers, London, 1984, p. 90.
28 H. Wang, Y.-I. Jang and Y.-M. Chiang, *Electrochem. Solid State Lett.*, 1999, **2**, 490.